

Fast MATLAB evaluation of nonlinear energies using FEM in 2D and 3D: nodal elements

Alexej Moskovka

Jan Valdman

Abstract

Nonlinear energy functionals appearing in the calculus of variations can be discretized by the finite element (FE) method and formulated as a sum of energy contributions from local elements. A fast evaluation of energy functionals containing the first order gradient terms is a central part of this contribution. We describe a vectorized implementation using the simplest P1 elements in which all energy contributions are evaluated all at once without the loop over triangular or tetrahedral elements. Furthermore, in connection to the first-order optimization methods, the discrete gradient of the energy functional is assembled in a way that gradient components are evaluated over all degrees of freedom all at once. The key ingredient is the vectorization of exact or approximate energy gradients over nodal patches. It leads to a time-efficient implementation at higher memory-cost. Provided codes in MATLAB related to 2D/3D hyperelasticity and 2D p-Laplacian problem are available for download and structured in a way it can be easily extended to other types of vector or scalar forms of energies.

1 Introduction

Given a domain $\Omega \in \mathbb{R}^{dim}$, where $dim \in \{1, 2, 3\}$ is the space-dimension, we consider a minimization problem

$$J(\mathbf{u}) = \min_{\mathbf{v} \in V} J(\mathbf{v}), \quad (1)$$

where V is a space of trial functions and $J : V \rightarrow \mathbb{R}$ represents an energy functional. The energy functional is assumed in the form

$$J(\mathbf{v}) = J_{grad}(\mathbf{v}) + J_{lin}(\mathbf{v}), \quad (2)$$

where $J_{grad}(\mathbf{v})$ denote the first-gradient part and $J_{lin}(\mathbf{v})$ the linear part of the energy functional, respectively. Examples of such minimization problems are numerous and their study is a general subject of Calculus of variations. There are models with higher order derivatives (such as plate problems with the second derivative in their formulation) available but not considered in this contribution.

As the main example we recall a class of vector nonlinear elasticity problems represented by minimizations of energies of hyperelastic materials [8, 10]. The trial space is chosen as

$$V = W_D^{1,p}(\Omega, \mathbb{R}^{dim})$$

i.e., the (vector) Sobolev space of $L^p(\Omega)$ integrable functions with the first weak derivative being also $L^p(\Omega)$ integrable and satisfying (in sense of traces) Dirichlet boundary conditions $\mathbf{v}(\mathbf{x}) = \mathbf{u}_D(\mathbf{x})$ at the domain boundary $\mathbf{x} \in \partial\Omega$ for a prescribed function $\mathbf{u}_D : \partial\Omega \rightarrow \mathbb{R}^{dim}$. A

primal variable is a deformation mapping $\mathbf{v} : \Omega \rightarrow \mathbb{R}^{dim}$ describing the relocation of any point $\mathbf{x} \in \Omega$ during the deformation process. Then the gradient deformation tensor is defined as

$$\mathbf{F}(\mathbf{v}) = \nabla \mathbf{v} = \begin{bmatrix} \frac{\partial v^{(1)}}{\partial x_1} & \cdots & \frac{\partial v^{(1)}}{\partial x_{dim}} \\ \vdots & & \vdots \\ \frac{\partial v^{(dim)}}{\partial x_1} & \cdots & \frac{\partial v^{(dim)}}{\partial x_{dim}} \end{bmatrix}$$

The concept of a strain is used to evaluate how much a given deformation differs locally from a rigid body deformation and the corresponding Green-Lagrangian strain tensor is defined as $\mathbf{E}(\mathbf{v}) = \frac{1}{2}(\mathbf{C}(\mathbf{v}) - \mathbf{I})$, where $\mathbf{C}(\mathbf{v}) = \mathbf{F}^T(\mathbf{v})\mathbf{F}(\mathbf{v})$ denotes the right Cauchy-Green deformation tensor and $\mathbf{I} \in \mathbb{R}^{dim \times dim}$ is an identity matrix. The energy functional is defined as

$$J_{grad}(\mathbf{v}) = \int_{\Omega} W(\mathbf{F}(\mathbf{v}(\mathbf{x}))) \, d\mathbf{x}, \quad J_{lin}(\mathbf{v}) = \int_{\Omega} \mathbf{f}(\mathbf{x}) \cdot \mathbf{v}(\mathbf{x}) \, d\mathbf{x}.$$

The gradient part is defined by a specified strain-energy density function $W(\cdot)$ including for instance the compressible Neo-Hookean density

$$W(\mathbf{F}) = C_1(I_1(\mathbf{F}) - dim - 2 \log(J(\mathbf{F}))) + D_1(J(\mathbf{F}) - 1)^2. \quad (3)$$

Here, $I_1(\mathbf{F}) = |\mathbf{F}|^2$, where $|\cdot|$ denotes the Frobenius norm, $J(\mathbf{F}) = \det \mathbf{F}$, where \det denotes the matrix determinant. The linear part assumes a loading functional $\mathbf{f} : \Omega \rightarrow \mathbb{R}^{dim}$. An extension to other gradient densities as the St. Venant Kirchhoff is possible.

As the second example we recall the scalar p-Laplacian problem [6] with the energy functional defined as

$$J(v) = \frac{1}{p} \int_{\Omega} |\nabla v(\mathbf{x})|^p \, d\mathbf{x} - \int_{\Omega} f(\mathbf{x}) v(\mathbf{x}) \, d\mathbf{x}, \quad (4)$$

where $V = W_D^{1,p}(\Omega, \mathbb{R})$. The functional $J(v)$ is then known to be strictly convex in V for $p \in [1, \infty)$ and it has therefore a unique minimizer $u(\mathbf{x}) \in V$.

The main motivation of this contribution is to describe how nonlinear energy functionals can be efficiently evaluated by the finite element method (FE). We provide vectorization concepts and MATLAB implementations of

- the energy value $J(\mathbf{v})$
- the gradient vector of the energy $J(\mathbf{v})$

expressed for a trial function $\mathbf{v} \in V$. There are not explicit loops over mesh elements known from finite element assemblies, all necessary data is computed all at once. It leads to significant computations speedup but also it is memory intensive. Then, these objects can be passed to an external optimization method of the first order. This is chosen as the trust-region method [3] in our MATLAB tests. There is already a growing number of vectorized implementations of linear second order partial differential equations eg. [7, 15]. We build our implementation on the top of own vectorized codes [2, 5, 13].

Authors are now aware of a simple MATLAB implementation that computes minima of non-quadratic energies corresponding to solutions of nonlinear partial differential equation. This is our first attempt in this direction. In a set of benchmarks we set up a base for future improvements. The user needs to specify the form of the energy $J(\mathbf{v})$. The corresponding gradient vector $\nabla J(\mathbf{v})$ is evaluated approximately from a central difference scheme. Alternatively, if the user is ready to apply some differential calculus to a particular form of the energy,

then the exact gradient can be assembled. It leads in our experiments to further improved performance.

The paper is structured in the following way: Section 2 summarizes useful notation and Section 3 basics of finite element discretization. Section 4 includes implementation of two structures further need: mesh and patches. Section 5 is focused on implementation of energy evaluation and Section 6 on implementation of the gradient of energy. The final Section 7 report of solutions of particular minimization problems: 2D/3D hyperelasticity and 2D p-Laplacian.

2 Notation

Domain triangulations are described by parameters:

$\mathcal{T}, \mathcal{N}, \mathcal{M}$ - a set of elements, a set of nodes, a set of (at least partially) free nodes

$\mathcal{T}^i, \mathcal{T}^{(n)}$ - the i -th nodal patch, the $(I_{DN}(n))$ -th nodal patch

Both scalar and vector problems are treated together as a vector problem with d components, where $d = 1$ for scalar problems, $d = \dim$ for vector problems and \dim is the space dimension. The following indices are frequently used:

i - an index of node ($i \in \{1, \dots, n_b\}$, also $i \in \{1, \dots, |\mathcal{N}|\}$ or $i \in \{1, \dots, |\mathcal{M}|\}$)

j - an index of vector component ($j \in \{1, \dots, d\}$)

k - an index of element ($k \in \{1, \dots, |\mathcal{T}|\}$, also $(k \in \{1, \dots, |\mathcal{T}^i|\})$ or $(k \in \{1, \dots, |\mathcal{T}^{(n)}|)$)

ℓ - an index of local basis function ($\ell \in \{1, \dots, \dim + 1\}$)

m - an index of spatial component ($m \in \{1, \dots, \dim\}$)

n - an index of global degree of freedom ($n \in \{1, \dots, d|\mathcal{N}|\}$) or active degree of freedom ($n \in \{1, \dots, d|\mathcal{M}|\}$)

r - an index of global patches matrix row ($r \in \{1, \dots, |\mathcal{M}|\}$)

Nodal basis functions are used in several ways:

$\varphi_i(\mathbf{x}), \boldsymbol{\varphi}_i(\mathbf{x})$ - a scalar global nodal basis function, a vector global nodal basis functions

$\varphi_{k,\ell}(\mathbf{x})$ - a local ℓ -th basis function on the k -th element

A trial vector function is addressed in several ways:

$\mathbf{v}(\mathbf{x}), v^{(j)}(\mathbf{x})$ - a trial vector function and its j -th component

\mathbf{V} - a matrix of coefficients of $\mathbf{v}(\mathbf{x})$ in the nodal finite element basis

$\mathbf{v}_i, \mathbf{v}^{(j)}, v_i^{(j)}$ - the i -th row of \mathbf{V} , the j -th column of \mathbf{V} , the (i,j) element of \mathbf{V}

\mathbf{v} - a vector reshaped from \mathbf{V}

$\hat{\mathbf{v}}$ - the restriction of \mathbf{v} to free nodes

Given matrices $\mathbf{A}, \mathbf{B} \in \mathbb{R}^{p \times q}$, the following operators are used:

$\text{tr}(\mathbf{A})$ - the trace of matrix

$\det(\mathbf{A})$ - the determinant of matrix

$\mathbf{A} : \mathbf{B}$ - the scalar product of matrices

$\mathbf{A} \odot \mathbf{B}$ - the elementwise product

Index mappings:

$I_{LG} : \mathbb{N} \rightarrow \mathbb{N}$ - (local to global) mapping which for a local basis function on the element returns the index of the corresponding global basis function

$I_{DN} : \mathbb{N} \rightarrow \mathbb{N}$ - (degree to node) mapping which for the n -th (active) degree of freedom returns the index i of the corresponding (free) node

3 Finite element discretization

The finite element method [4] is applied for a discretization of (1). We assume the trial function and the trial space of the form

$$\mathbf{v}(\mathbf{x}) = (v^{(1)}(\mathbf{x}), \dots, v^{(d)}(\mathbf{x})), \quad V = V^{(1)} \times \dots \times V^{(d)}.$$

and approximate $\mathbf{v}(\mathbf{x}) \in V$ in the finite-dimensional subspace

$$V_h = V_h^{(1)} \times \dots \times V_h^{(d)} \subset V,$$

where $V_h^{(1)} = \dots = V_h^{(d)} := V_h^s$ and a scalar basis space V_h^s is generated from scalar basis functions

$$\varphi_i(\mathbf{x}) \in V_h^s, \quad i \in \{1, \dots, n_b\},$$

where n_b denotes their number. Hence, any component of $\mathbf{v}(\mathbf{x})$ is given by a linear combination

$$v^{(j)}(\mathbf{x}) = \sum_{i=1}^{n_b} v_i^{(j)} \varphi_i(\mathbf{x}), \quad \mathbf{x} \in \Omega, \quad j \in \{1, \dots, d\}. \quad (5)$$

Coefficients $v_i^{(j)}$ from (5) are assembled in a matrix $\mathbf{V} \in \mathbb{R}^{n_b \times d}$ given as

$$\mathbf{V} = \begin{pmatrix} v_1^{(1)} & \dots & v_1^{(d)} \\ \vdots & & \vdots \\ \vdots & & \vdots \\ v_{n_b}^{(1)} & \dots & v_{n_b}^{(d)} \end{pmatrix} = \begin{pmatrix} \mathbf{v}_1 \\ \vdots \\ \mathbf{v}_{n_b} \end{pmatrix} = (\mathbf{v}^{(1)} \dots \mathbf{v}^{(d)}) \quad (6)$$

and latter two equivalent forms assume a row vector $\mathbf{v}_i = (v_i^{(1)}, \dots, v_i^{(d)})$, $i \in \{1, \dots, n_b\}$ and a column vector $\mathbf{v}^{(j)} = (v_1^{(j)}, \dots, v_{n_b}^{(j)})^T$, $j \in \{1, \dots, d\}$. Using a row vector basis function

$$\varphi_i(\mathbf{x}) = \underbrace{(\varphi_i(\mathbf{x}), \dots, \varphi_i(\mathbf{x}))}_{d \text{ - times}}, \quad i \in \{1, \dots, n_b\}$$

one can rewrite (5) in a compact way for all components $j \in \{1, \dots, d\}$ as

$$\mathbf{v}(\mathbf{x}) = \sum_{i=1}^{n_b} \mathbf{v}_i \odot \varphi_i(\mathbf{x}), \quad \mathbf{x} \in \Omega, \quad (7)$$

where the symbol \odot represents an elementwise multiplication [14] (here multiplication of components with the same index j). The formula (7) is a key tool to a vectorized implementation, since MATLAB provides the elementwise multiplication.

The domain Ω is then approximated by its triangulation \mathcal{T} into closed elements in the sense of Ciarlet. The simplest possible elements are considered, i.e., intervals for $\dim = 1$, triangles for $\dim = 2$ and tetrahedra for $\dim = 3$. The elements are geometrically specified by its nodes (or vertices) belonging to the set of nodes \mathcal{N} . Nodes are also clustered into elements edges (for $\dim \geq 2$) and faces (for $\dim = 3$). Numbers of elements and of nodes are denoted as $|\mathcal{T}|$ and $|\mathcal{N}|$. Given a node $N_i \in \mathcal{N}, i \in \{1, \dots, |\mathcal{N}|\}$, we define a nodal patch by $\mathcal{T}^i = \{T \in \mathcal{T} : N_i \in T\}$ and the number of its elements by $|\mathcal{T}^i|$. The nodal patch \mathcal{T}^i consists of elements $T_k^i, k \in \{1, \dots, |\mathcal{T}^i|\}$ adjacent to the node N_i . We consider only the case, where $V_h^s = P^1(\mathcal{T})$ is the space of nodal, elementwise linear and globally continuous scalar functions. Then number of basis function is equal to number of nodes,

$$n_b = |\mathcal{N}|,$$

but some coefficients of the trial function $\mathbf{v}(\mathbf{x})$ are known due to the Dirichlet boundary conditions.

Example 1 One regular triangulation \mathcal{T} of the L-shape domain Ω is shown in Fig. 1. The triangulation is specified by $|\mathcal{T}| = 24$ and $|\mathcal{N}| = 21$. The graph of the global scalar basis function $\varphi_{10}(\mathbf{x})$ is displayed. The function has a hexagonal pyramid shape and a support on the nodal patch $\mathcal{T}^{10} = \{T_1, T_2, T_7, T_8, T_{19}, T_{20}\}$. Restrictions of $\varphi_{10}(\mathbf{x})$ to its six supporting triangles in \mathcal{T}^{10} are given as linear functions with values 1 at the node N_{10} and values 0 at two remaining nodes.

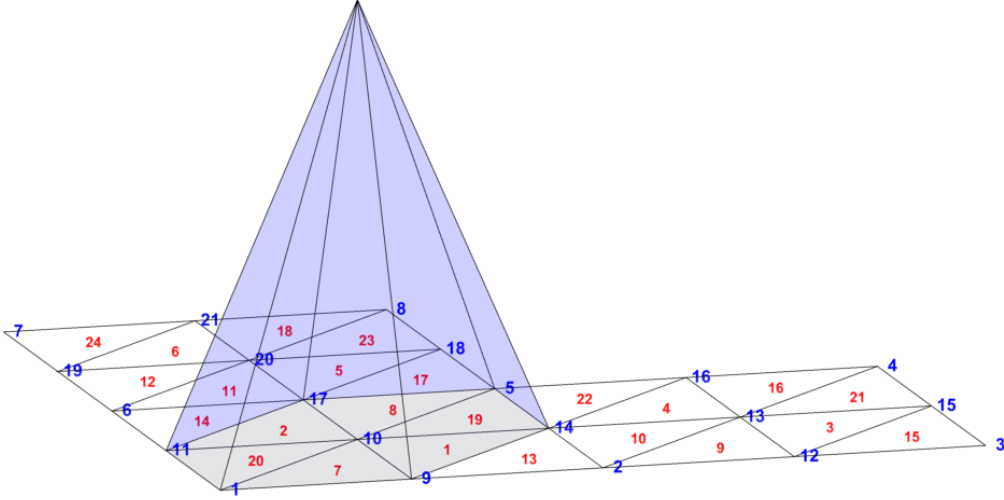


Figure 1: Example of a scalar nodal basis function for $\dim = 2$.

3.1 The first-gradient energy term $J_{grad}(\mathbf{v})$

Since the first-gradient of any scalar basis function $\varphi_i(\mathbf{x}) \in P^1(\mathcal{T}), i \in \{1, \dots, |\mathcal{N}|\}$ is a piecewise constant function on each element, the gradient part of the discrete energy can be written as a

sum over elements

$$J_{grad}(\mathbf{v}) = \int_{\Omega} W(\mathbf{F}(\mathbf{v}(\mathbf{x}))) \, d\mathbf{x} = \sum_{k=1}^{|\mathcal{T}|} \int_{T_k} W(\nabla \mathbf{v}(\mathbf{x})) \, d\mathbf{x} = \sum_{k=1}^{|\mathcal{T}|} |T_k| W(\nabla \mathbf{v}(\mathbf{x})|_{T_k}), \quad (8)$$

and $|T_k|$ denotes the size of the element T_k , $k \in \{1, \dots, |\mathcal{T}|\}$ (equal to its length in 1D, its area in 2D or its volume in 3D). In order to evaluate (8), we need to assemble the gradient $\mathbf{v}(\mathbf{x})|_{T_k}$ on every element. To do it, we define a (local-global) mapping $I_{LG} : \mathbb{N} \times \mathbb{N} \rightarrow \mathbb{N}$ which for the k -th element and its ℓ -th node returns the global index i of this node. Then a local basis function is given as

$$\varphi_{k,\ell}(x) = \varphi_i|_{T_k}(x), \quad \text{where } i = I_{LG}(k, \ell) \quad (9)$$

for $k \in \{1, \dots, |\mathcal{T}|\}$, $\ell \in \{1, \dots, \dim + 1\}$. Hence, any of partial derivatives of $\mathbf{v}(\mathbf{x})$ with respect to x_m read

$$\left. \frac{\partial \mathbf{v}(\mathbf{x})}{\partial x_m} \right|_{T_k} = \sum_{\ell=1}^{\dim+1} \mathbf{v}_{k,\ell} \odot \frac{\partial \varphi_{k,\ell}(\mathbf{x})}{\partial x_m}, \quad m \in \{1, \dots, \dim\}, \quad (10)$$

where $\mathbf{v}_{k,\ell} = \mathbf{v}_{I_{LG}(k,\ell)}$ represents values of \mathbf{v} in the ℓ -th node of the k -th element.

3.2 The linear energy term J_{lin}

Furthermore, if $\mathbf{f}(\mathbf{x}) \in V_h$, then the linear term of the energy (2) rewrites as

$$\begin{aligned} J_{lin}(\mathbf{v}) &= \int_{\Omega} \mathbf{f}(\mathbf{x}) \cdot \mathbf{v}(\mathbf{x}) \, d\mathbf{x} = \sum_{j=1}^d \int_{\Omega} f^{(j)}(\mathbf{x}) v^{(j)}(\mathbf{x}) \, d\mathbf{x} = \\ &= \sum_{j=1}^d \int_{\Omega} \left(\sum_{i_1=1}^{|\mathcal{N}|} f_{i_1}^{(j)} \varphi_{i_1}(\mathbf{x}) \sum_{i_2=1}^{|\mathcal{N}|} v_{i_2}^{(j)} \varphi_{i_2}(\mathbf{x}) \right) d\mathbf{x} = \\ &= \sum_{j=1}^d \sum_{i_1=1}^{|\mathcal{N}|} \sum_{i_2=1}^{|\mathcal{N}|} f_{i_1}^{(j)} v_{i_2}^{(j)} \int_{\Omega} \left(\varphi_{i_1}(\mathbf{x}) \varphi_{i_2}(\mathbf{x}) \right) d\mathbf{x}. \end{aligned} \quad (11)$$

All integral terms in the formula above can be assembled in a sparse and symmetric mass matrix $\mathbf{M} \in \mathbb{R}^{|\mathcal{N}| \times |\mathcal{N}|}$ with entries

$$\mathbf{M}_{i_1, i_2} = \int_{\Omega} \varphi_{i_1}(\mathbf{x}) \varphi_{i_2}(\mathbf{x}) \, d\mathbf{x}, \quad i_1, i_2 \in \{1, 2, \dots, |\mathcal{N}|\}. \quad (12)$$

Then we can define vectors $\mathbf{b}^{(j)} = \mathbf{M} \mathbf{f}^{(j)} \in \mathbb{R}^{|\mathcal{N}|}$, where $\mathbf{f}^{(j)} = (f_1^{(j)}, \dots, f_{|\mathcal{N}|}^{(j)})^T \in \mathbb{R}^{|\mathcal{N}|}$, $j \in \{1, \dots, d\}$ and it is easy to check the exact formula

$$J_{lin}(\mathbf{v}) = \int_{\Omega} \mathbf{f}(\mathbf{x}) \cdot \mathbf{v}(\mathbf{x}) \, d\mathbf{x} = \sum_{j=1}^d \mathbf{b}^{(j)} \cdot \mathbf{v}^{(j)}, \quad (13)$$

which allows us to represent the linear part of the discrete energy $J(\mathbf{v})$ as a linear function.

4 Implementation: Mesh and nodal patches

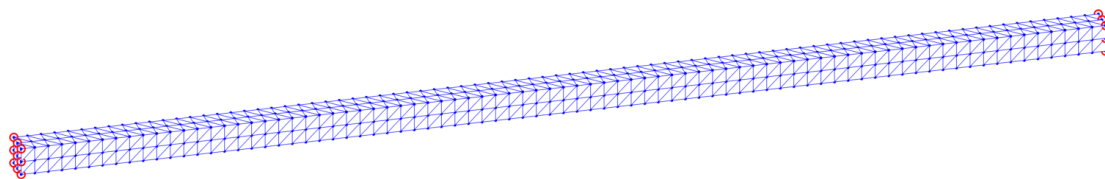


Figure 2: Example: A tetrahedral mesh of a 3D bar domain with red boundary nodes.

4.1 A mesh structure

Considered finite element meshes consist of triangles (in 2D) and tetrahedra (in 3D). We describe typical properties of meshes and basic tools needed in our computational techniques.

The topology and important attributes of the computational domain are stored in a structure-type data object `'mesh'`. For an example of a tetrahedral mesh displayed in Fig. 2, a vector energy model and full Dirichlet boundary conditions (specified in all three directions and indicated by nodes in red circles) it provides the following information:

```
mesh =

  struct with fields:

      dim: 3
      level: 1
      nn: 729
      ne: 1920
      elems2nodes: [1920×4 double]
      nodes2coord: [729×3 double]
      volumes: [1920×1 double]
      dphi: {[1920×4 double] [1920×4 double] [1920×4 double]}
      nodesDirichlet: [18×1 double]
      nodesMinim: [711×1 double]
      dofsDirichlet: [54×1 double]
      dofsMinim: [2133×1 double]
```

The parameter `'dim'` represents the domain dimension (here equal to 3) of the problem and `'level'` a level of uniform refinement. Higher levels of refinement lead to finer uniformly refined meshes with more elements. Numbers of mesh nodes and elements are provided in `'nn'` and `'ne'`. Mesh nodes belonging to each tetrahedron are collected in a matrix `'elems2nodes'` and Cartesian coordinates of mesh nodes in a matrix `'nodes2coord'`.

Once last two matrices are given, the codes of [13] generate `'volumes'` of all tetrahedra together with restrictions of partial derivatives (gradients) of all P1-basis functions to tetrahedra stored in a cell `'dphi'` whose components are three matrices corresponding to the partial derivatives with respect to every x_m , $m \in \{1, \dots, dim\}$.

Indices of Dirichlet boundary nodes are stored in a vector `'nodesDirichlet'` and remaining free nodes in a vector `'nodesMinim'`. Vectors `'dofsDirichlet'` and `'dofsMinim'` denotes indices of degrees of freedom corresponding to Dirichlet and free nodes.

Remark 1 The vectors '*dofsDirichlet*' and '*dofsMinim*' are equal to vectors '*nodesDirichlet*' and '*nodesMinim*' in case of a scalar energy formulation.

4.2 A patches structure

This object is only relevant if the knowledge of gradient $\nabla J(\mathbf{v})$ is required, e.g. as an input of the trust-region method of Section 7. Then, an additional structure-type data object '**patches**' is constructed for the evaluation of its gradient part given by (8).

Remark 2 Only the components of $\nabla J(\mathbf{v})$ corresponding to the free nodes are evaluated in our implementation, and the remaining components belonging to the full Dirichlet boundary conditions are omitted. Thus, nodes with at least one free degree of freedom also belong to the set of free nodes, the gradient is evaluated in all their components and finally restricted to the free degrees of freedom.

We denote by \mathcal{M} the set of all free nodes and by $|\mathcal{M}|$ their number. Then, the node index $i, i \in \{1, \dots, |\mathcal{M}|\}$ goes exclusively through the free nodes. A nodal patch $\mathcal{T}^i, i \in \{1, \dots, |\mathcal{M}|\}$ is implemented as a vector of elements indices **elems_i**, a vector of their volumes **volumes_i**, a matrix of corresponding elements nodes stored as **elems2nodes_i**, values of gradients of local basis functions stores as a cell **dphi_i** with matrices components **dphi_i{1}**, **dphi_i{2}**, **dphi_i{3}**. All these matrices and vectors are of size $|\mathcal{T}^i| \times (dim + 1)$ and $|\mathcal{T}^i| \times 1$, respectively.

The data of all nodal patches $\mathcal{T}^i, i \in \{1, \dots, |\mathcal{M}|\}$ are then collected in long global matrices or vectors with the number of rows equal to

$$\|\mathcal{T}\| = \sum_{i=1}^{|\mathcal{M}|} |\mathcal{T}^i|.$$

If we define for $i \in \{1, \dots, |\mathcal{M}|\}$ indices

$$p_0 = 0, \quad p_i = \sum_{r=1}^i |\mathcal{T}^r|, \quad (14)$$

then the submatrix or subvector extracted from the rows $(p_{i-1} + 1), \dots, p_i$ of the global matrices or the vector above corresponds to the i -th nodal patch. It is shown schematically in Figure 3. Thus we obtain the global vectors **elems**, **volumes** of size $\|\mathcal{T}\| \times 1$ and the global matrices **elems2nodes**, **dphi{1}**, **dphi{2}**, **dphi{3}**, of size $\|\mathcal{T}\| \times (dim + 1)$.

Remark 3 For the gradient evaluation of Section 6 we will need to extend the set of $p_i, i \in \{0, \dots, |\mathcal{M}|\}$ indices up to $\{0, \dots, d|\mathcal{M}|\}$. Thus, we define additionally

$$\begin{aligned} p_n &= p_{n-|\mathcal{M}|} + \|\mathcal{T}\|, & n &\in \{|\mathcal{M}| + 1, \dots, 2|\mathcal{M}|\} \\ p_n &= p_{n-2|\mathcal{M}|} + 2\|\mathcal{T}\|, & n &\in \{2|\mathcal{M}| + 1, \dots, 3|\mathcal{M}|\} \end{aligned} \quad (15)$$

In order to maintain the right ordering of local basis functions within each nodal patch, an additional logical-type matrix of zeros and ones **logical** is provided. If the n -th row corresponds to the i -th patch, then **logical**(n, ℓ) = 1 means that **elems2nodes**(n, ℓ) = i . Therefore, in every row of **logical** matrix value '1' has exactly one single occurrence.

Below we provide an example of '**patches**' structure along with the same '**mesh**' one introduced in Subsection 4.1 and corresponding to the domain in Fig. 2.

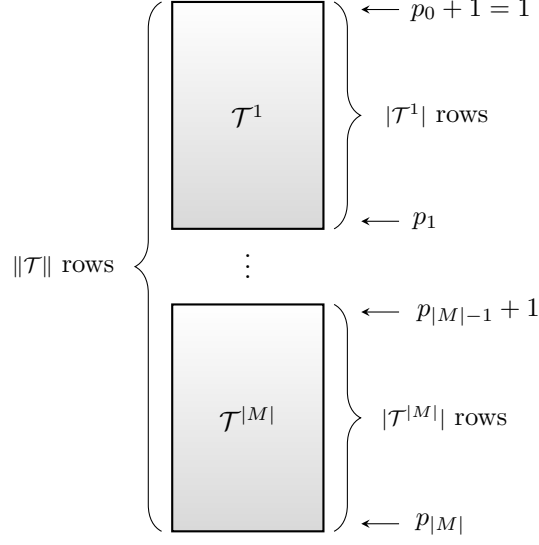


Figure 3: All data from nodal patches are stored in long matrices or vectors.

`patches =`

`struct with fields:`

```

    lengths: [711×1 double]
      elems: [7584×1 double]
    volumes: [7584×1 double]
  elems2nodes: [7584×4 double]
        dphi: {[7584×4 double] [7584×4 double] [7584×4 double]}
    logical: [7584×4 logical]

```

The first vector **lengths** is of size $|\mathcal{M}| \times 1$ with entries $\mathbf{lengths}(i) = |\mathcal{T}^i|$, $i \in \{1, \dots, |\mathcal{M}|\}$. Here, its size is equal to $711 = 729 - 18$, where $|\mathcal{N}| = 729$ is the number of mesh nodes and 18 is the number of nodes with full Dirichlet boundary conditions.

Benchmark 1 *The script `benchmark1.m` generates a sequence of structures `mesh` and `patches` corresponding to each of uniform mesh refinements. Table 1 provides assembly times and memory requirements of both objects.*

mesh level	number of nodes $ \mathcal{N} $	number of elems. $ \mathcal{T} $	number of free dofs	mesh setup time [s]	patches setup time [s]	mesh memory size [MB]	patches memory size [MB]
1	729	1920	2133	0.02	0.01	0.47	1.13
2	4025	15360	11925	0.03	0.02	3.28	9.07
3	26001	122880	77517	0.36	0.15	24.55	72.73
4	185249	983040	554013	2.36	1.16	189.88	582.53
5	1395009	7864320	4178493	23.30	11.54	1493.38	4663.18

Table 1: Benchmark 1 - setup times and memory consumption in 3D.

*Note that the most memory consuming part of both structures is given by substructures **dphi** containing values of precomputed gradients of basis functions.*

5 Implementation: energy evaluation

The following matrix-vector transformation is frequently used: matrices $\mathbf{B}, \mathbf{V} \in \mathbb{R}^{|\mathcal{N}| \times d}$ are stretched to isomorphic vectors

$$\mathbf{b}, \mathbf{v} \in \mathbb{R}^{d|\mathcal{N}|} : \quad \mathbf{b}_n = \mathbf{B}_{i,j}, \quad \mathbf{v}_n = \mathbf{V}_{i,j}, \quad n \in \{1, \dots, d|\mathcal{N}|\}, \quad (16)$$

where $i = (n-1)/d + 1$ and $j = (n-1)\%d + 1$. Here, $/$ symbol is the integer division operator and $\%$ is the modulo operator. Put simply, for any $i \in \{1, \dots, |\mathcal{N}|\}$ the elements of \mathbf{v} with indices $d(i-1) + 1, \dots, d(i-1) + d$ corresponds to the values of the trial function $\mathbf{v}(\mathbf{x})$ in the i -th node in directions $1, \dots, d$.

5.1 The linear energy term J_{lin}

The linear part of the energy (13) rewrites equivalently as

$$J_{lin}(\mathbf{v}) = \int_{\Omega} \mathbf{f}(\mathbf{x}) \cdot \mathbf{v}(\mathbf{x}) \, d\mathbf{x} = \mathbf{B} : \mathbf{V} = \mathbf{b} \cdot \mathbf{v}, \quad (17)$$

where $:$ denotes the scalar product of matrices.

5.2 The first-gradient energy term J_{grad}

The gradient part of the discrete energy (8) is given as the sum of energy contributions from every element T_k , $k \in \{1, \dots, |\mathcal{T}|\}$ and its evaluation in MATLAB is performed effectively by using operations with vectors and matrices only. The energy evaluation for a trial vector $\mathbf{v} \in \mathbb{R}^{d|\mathcal{N}|}$ is performed by the main function:

```

1 function [e, densities] = energy(v, mesh, params)
2 % components of deformation
3 v_cell = createCellFromVector(v, mesh.dim);
4
5 % components of deformation on elements
6 v_elems = CellAtMatrixOfIndices(v_cell, mesh.elems2nodes);
7
8 % deformation gradients on elements

```

```

9  F_elems = evaluate_F(mesh, v_elems);
10
11 % gradient densities on elements
12 densities.Gradient = densityGradientVector_3D(F, params);
13
14 % total gradient energy
15 e = sum(mesh.volumes.*densities.Gradient);
16 end

```

where $\mathbf{b} \in \mathbb{R}^{d|\mathcal{N}|}$ is defined in (16) and precomputed, **mesh** is described in section 5 and **params** contain material parameters apart from some other parameters (e.g. visualization parameters). The code above is vectorized and generates the objects:

A cell **v_elems** containing matrices **v_elems**{1}, **v_elems**{2}, **v_elems**{3} of size $|\mathcal{T}| \times 4$ providing restrictions of nodal deformations to all elements.

A cell **F** of size $\dim \times \dim$ storing the deformation gradients in all elements. In particular, **F**{ d }{ m } is then a vector of size $|\mathcal{T}| \times 1$ evaluating partial derivatives of the d -th component of deformation with respect to the m -th variable in all elements.

A vector **densities.Gradient** of size $|\mathcal{T}| \times 1$ containing gradient densities in all elements.

The energy **e** is given as the sum of gradient energy contributions over elements (the gradient part $J_{grad}(\mathbf{v})$ given by (8)) subtracted by the linear energy term $J_{lin}(\mathbf{v})$ (given by (13)).

The Neo-Hook density function $W = W(F)$ from (3) is implemented as

```

1  function densities=densityGradientVector_3D(F, params)
2  % J term (determinant)
3  J = F{1,1}.*F{2,2}.*F{3,3} + F{1,3}.*F{2,1}.*F{3,2} + ...
4      F{1,2}.*F{2,3}.*F{3,1} - F{1,3}.*F{2,2}.*F{3,1} - ...
5      F{1,2}.*F{2,1}.*F{3,3} - F{1,1}.*F{2,3}.*F{3,2};
6
7  % I1 term (Frobenius norm squared)
8  I1 = F{1,1}.^2 + F{1,2}.^2 + F{1,3}.^2 + ...
9      F{2,1}.^2 + F{2,2}.^2 + F{2,3}.^2 + ...
10     F{3,1}.^2 + F{3,2}.^2 + F{3,3}.^2;
11
12 % gradient densities
13 densities = params.C1*(I1-3-2*log(J)) + params.D1*(J-1).^2;
14 end

```

Benchmark 2 Assume the bar domain $\Omega = (0, l_x) \times (-\frac{l_y}{2}, \frac{l_y}{2}) \times (-\frac{l_z}{2}, \frac{l_z}{2})$, where $l_x = 0.4, l_y = l_z = 0.01$, specified by the material parameters $E = 2 \cdot 10^8$ (Young's modulus) and $\nu = 0.3$ (Poisson's ratio) and deformed by the prescribed deformation $\mathbf{v}(\mathbf{x}) = \mathbf{v}(x, y, z)$ given by

$$\begin{aligned}
v^{(1)}(x, y, z) &= x, \\
v^{(2)}(x, y, z) &= \cos(\alpha \frac{x}{l_x}) y + \sin(\alpha \frac{x}{l_x}) z, \\
v^{(3)}(x, y, z) &= -\sin(\alpha \frac{x}{l_x}) y + \cos(\alpha \frac{x}{l_x}) z,
\end{aligned} \tag{18}$$

or equivalently using matrix operations

$$\begin{pmatrix} v^{(1)}(x, y, z) \\ v^{(2)}(x, y, z) \\ v^{(3)}(x, y, z) \end{pmatrix} = \begin{pmatrix} 1 & 0 & 0 \\ 0 & \cos(\alpha \frac{x}{l_x}) & \sin(\alpha \frac{x}{l_x}) \\ 0 & -\sin(\alpha \frac{x}{l_x}) & \cos(\alpha \frac{x}{l_x}) \end{pmatrix} \begin{pmatrix} x \\ y \\ z \end{pmatrix}. \tag{19}$$

Here, $\alpha = 2\pi$ means that the right Dirichlet wall is twisted once around the x -axes (Fig. 4). Constants C_1, D_1 are transformed according to formulas $C_1 = \frac{\nu}{2}, D_1 = \frac{K}{2}$, where $K = \frac{E}{3(1-2\nu)}$ is the bulk modulus. The exact evaluation shows that the corresponding gradient energy using the Neo-Hookean density function (3) reads

$$J_{grad}(\mathbf{v}) \approx 6.326670.$$

The script `benchmark2.m` evaluates approximation of $J_{grad}(\mathbf{v})$ on a sequence of uniform mesh refinements defined in Benchmark 1. In order to provide higher accuracy of measure evaluation times, the energies are recomputed 100 times. Table 2 provides evaluation times and values of the energy approximations.

mesh level	number of free dofs	evaluation (100x) of $J_{grad}(\mathbf{v})$: time [s]	value of $J_{grad}(\mathbf{v})$
1	2133	0.04	12.6623
2	11925	0.19	7.9083
3	77517	1.22	6.7219
4	554013	9.31	6.4255
5	4178493	176.94	6.3514

Table 2: Benchmark 2 - energy evaluation times in 3D.

6 Implementation: energy gradient evaluation

Evaluation of the full gradient $\nabla J(\mathbf{v})$, where $\mathbf{v} = (v_1, \dots, v_{d|\mathcal{N}|}) \in \mathbb{R}^{d|\mathcal{N}|}$, requires in general computation of all partial derivatives $\frac{\partial J(\mathbf{v})}{\partial v_n}$, $n \in \{1, \dots, d|\mathcal{N}|\}$. Minimization methods (e.g. trust-region mentioned applied in Section 7) require the knowledge of gradient, but only restricted to the free degrees of freedom.

The gradient $\nabla J_{lin}(\mathbf{v})$ easily reads using (17)

$$\nabla J_{lin}(\mathbf{v}) = \mathbf{b}, \quad (20)$$

where \mathbf{b} is of size $d|\mathcal{N}|$, given by (16) and its restriction to the free degrees of freedom is then trivial.

The evaluation of $\nabla J_{grad}(\mathbf{v})$ is more involving. With respect to Remark 2, $J_{grad}(\mathbf{v})$ is evaluated in our implementation for all degrees of freedom belonging to all (at least partially) free nodes are then restricted to the free degrees of freedom. In order to determine to which node the n -th active degree of freedom belongs we define the index mapping

$$I_{DN} : \{1, \dots, d|\mathcal{M}|\} \rightarrow \{1, \dots, |\mathcal{M}|\}, \quad I_{DN}(n) = (n-1)/d + 1$$

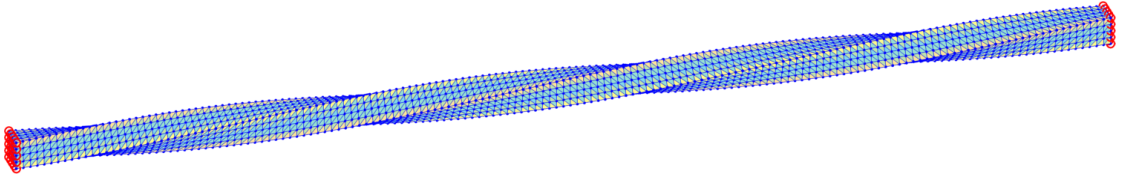


Figure 4: A bar domain twisted by the prescribed deformation (18).

which for the n -th active degree of freedom returns the corresponding i -th free node (here $/$ is an integer division operator). By

$$\mathcal{T}^{(n)}, \quad n \in \{1, \dots, d|\mathcal{M}|\}$$

we denote the set of elements adjacent to the node $N_{IDN(n)}$ belonging to the n -th active degree of freedom and by $|\mathcal{T}^{(n)}|$ their number. The gradient of the nonlinear part $J_{grad}(\mathbf{v})$ can be computed in two different ways:

1. numerically, where the partial derivatives are computed approximately by using a difference scheme.
2. exactly by taking the explicit partial derivatives.

Deriving the exact partial derivatives can be demanding and it depends on the particular problem. On the contrary, the numerical approach is more general and is feasible regardless of the complexity of the function representing the corresponding discrete energy. Hence, we first describe the numerical approach by using the central difference scheme and then explain the gradient evaluation by deriving the explicit form of partial derivatives.

6.1 Numerical approach to evaluate $\nabla J_{grad}(\mathbf{v})$

By using the central difference scheme, one can write

$$\frac{\partial}{\partial v_n} J_{grad}(\mathbf{v}) \approx \frac{J_{grad}(\mathbf{v} + \varepsilon \mathbf{e}_n) - J_{grad}(\mathbf{v} - \varepsilon \mathbf{e}_n)}{2\varepsilon},$$

where \mathbf{e}_n is the n -th canonical vector in $\mathbb{R}^{d|\mathcal{M}|}$ and ε is a small positive number. Both summands in the numerator above can be directly evaluated by taking the energy evaluation procedure introduced in the previous subsection as

$$\begin{aligned} J_{grad}(\mathbf{v} + \varepsilon \mathbf{e}_n) - J_{grad}(\mathbf{v} - \varepsilon \mathbf{e}_n) &= \\ &= \sum_{k=1}^{|\mathcal{T}|} \int_{T_k} W(\nabla(\mathbf{v} + \varepsilon \mathbf{e}_n)) \, d\mathbf{x} - \sum_{k=1}^{|\mathcal{T}|} \int_{T_k} W(\nabla(\mathbf{v} - \varepsilon \mathbf{e}_n)) \, d\mathbf{x}. \end{aligned}$$

However, this approach is ineffective as long as the step of central difference scheme ε occurs only in a few summands of the sums representing $J_{grad}(\mathbf{v} + \varepsilon \mathbf{e}_n)$ and $J_{grad}(\mathbf{v} - \varepsilon \mathbf{e}_n)$ given by (8), while the remaining summands are the same and therefore vanish. Hence, we can further simplify

$$\begin{aligned} J_{grad}(\mathbf{v} + \varepsilon \mathbf{e}_n) - J_{grad}(\mathbf{v} - \varepsilon \mathbf{e}_n) &= \\ &= \sum_{k=1}^{|\mathcal{T}^{(n)}|} \int_{T_k^{(n)}} W(\nabla(\mathbf{v} + \varepsilon \mathbf{e}_n)) \, d\mathbf{x} - \sum_{k=1}^{|\mathcal{T}^{(n)}|} \int_{T_k^{(n)}} W(\nabla(\mathbf{v} - \varepsilon \mathbf{e}_n)) \, d\mathbf{x} = \\ &= \sum_{k=1}^{|\mathcal{T}^{(n)}|} |T_k^{(n)}| W(\nabla(\mathbf{v} + \varepsilon \mathbf{e}_n)|_{T_k^{(n)}}) - \sum_{k=1}^{|\mathcal{T}^{(n)}|} |T_k^{(n)}| W(\nabla(\mathbf{v} - \varepsilon \mathbf{e}_n)|_{T_k^{(n)}}). \end{aligned} \tag{21}$$

By using the substitution

$$J_{grad}^{(n),+}(\mathbf{v}) = |T_k^{(n)}| W(\nabla(\mathbf{v} + \varepsilon \mathbf{e}_n)|_{T_k^{(n)}}), \quad J_{grad}^{(n),-}(\mathbf{v}) = |T_k^{(n)}| W(\nabla(\mathbf{v} - \varepsilon \mathbf{e}_n)|_{T_k^{(n)}}), \tag{22}$$

one can rewrite (21)

$$J_{grad}(\mathbf{v} + \varepsilon \mathbf{e}_n) - J_{grad}(\mathbf{v} - \varepsilon \mathbf{e}_n) = \sum_{k=1}^{|\mathcal{T}^{(n)}|} J_{grad}^{(n),+}(\mathbf{v}) - \sum_{k=1}^{|\mathcal{T}^{(n)}|} J_{grad}^{(n),-}(\mathbf{v}) \quad (23)$$

and evaluate the whole $\nabla J_{grad}(\mathbf{v})$ via the simple for-loop over its components.

Remark 4 *The energy evaluation procedure has to be called in every loop over vector components $n \in \{1, \dots, d|\mathcal{M}|\}$ and it turned out to cause multiple self built-in times that slowed down the performance. To avoid that, the original energy evaluation procedure is modified so that multiple input vectors can be processed simultaneously and the energy evaluation procedure be called only once.*

The outer gradient evaluation procedure is simple:

```

1 eps = 1e-8; % finite difference step size
2
3 % local patch energies for +eps and -eps
4 es_minsplus = energies(v, [-eps eps], mesh, patches, params, indx);
5
6 % the gradient vector by the central difference scheme
7 g = diff(es_minsplus, 1, 2) / eps / 2;
```

Here **es_minsplus** is a matrix of size $3\|\mathcal{T}\| \times 2$ with components $\text{es_minsplus}(n, 1) = J_{grad}^{(n),-}(\mathbf{v})$, $\text{es_minsplus}(n, 2) = J_{grad}^{(n),+}(\mathbf{v})$ which are given by (22). The gradient vector **g** is then assembled by using the central difference scheme with a constant central difference step size ε for all $n \in \{1, \dots, d|\mathcal{M}|\}$. Obviously, a generalization of the above code to higher accuracy difference scheme are possible to be added.

We recall that in the energy evaluation procedure **energy** from Subsection 5.2 a cell **v_elems** containing matrices **v_elems**{1}, **v_elems**{2} and **v_elems**{3} of the same size $|\mathcal{T}| \times 4$ is assembled. For computing $J_{grad}(\mathbf{v})$ by using (23) we need to assemble a cell-structure **v_patches** instead containing matrices **v_patches**{1}, **v_patches**{2}, **v_patches**{3} of size $\|\mathcal{T}\| \times 4$ providing restrictions of nodal deformations to all patches.

The extended procedure **energies** evaluates all ε -perturbed values of energies:

```

1 function e = energies(v, eps, mesh, patches, params, indx)
2 % components of deformation
3 v_cell = createCellFromVector(v, mesh.dim);
4 % components of deformation on elements
5 v_elems = CellAtMatrixOfIndices(v_cell, mesh elems2nodes);
6 % deformation gradients on elements
7 F_elems = evaluate_F(mesh, v_elems);
8
9 % deformations on patches
10 v_patches = CellAtMatrixOfIndices(v_cell, patches elems2nodes);
11 % deformation gradients on patches
12 F_patches = CellAtMatrixOfIndices(F_elems, patches elems);
13
14 v_patches_eps = cell(3, 1);
15 e = zeros(3 * numel(mesh.nodesMinim), size(eps, 2));
16 for comp=1:size(eps, 2) % loop over epsilon perturbations
17     % perturbations of deformations on patches
```

```

18 v_patches_eps{1} = v_patches{1} + eps(comp)*patches.logical;
19 v_patches_eps{2} = v_patches{2} + eps(comp)*patches.logical;
20 v_patches_eps{3} = v_patches{3} + eps(comp)*patches.logical;
21
22 % deformation gradients of perturbation
23 GG = evaluate_GG(patches, v_patches_eps, F_patches);
24
25 % densities
26 densities_patches = densityGradientVector_3D(GG, params);
27 % energies
28 e_patches = [patches.volumes; patches.volumes; patches.volumes].*
              densities_patches;
29 % final energy values on patches
30 csep = cumsum(e_patches);
31 e([1:3:end 2:3:end 3:3:end], comp) = [csep(indx(1)); diff(csep(indx))];
32 end
33 e = e(mesh.dofsMinim_local, :); % dropping out the Dirichlet dofs
34 end

```

The cell **v_elems** is the same as in the first-gradient energy evaluation procedure from Section 5 and the **F_elems** here is the same as **F_elems** in the **energy** procedure. The cell **v_patches_eps** inside the loop has the same size as well as its components that provide restrictions of nodal deformations to all patches, but here these deformations are perturbed by the value of the central difference step ε . This cell is used for the construction of the key cell **GG** of size $dim \times dim$, where $\mathbf{GG}\{j, m\}$, $j \in \{1, \dots, d\}$, $m \in \{1, \dots, dim\}$ is a vector of length $dim \cdot \|\mathcal{T}\|$ containing the partial derivatives of deformations of the j -th component with respect to the m -th variable. The first $\|\mathcal{T}\|$ entries of this vector correspond to the ε -perturbation of the first components of deformations. Similarly, the following $\|\mathcal{T}\|$ values corresponds to the ε -perturbations of the second components of deformations and the last $\|\mathcal{T}\|$ ones corresponds to the ε -perturbations of the third component. A vector **cs** of length $d\|\mathcal{T}\|$ contains cumulative sums of **e_patches** with elements

$$\mathbf{cs}(n) = \sum_{r=1}^n \mathbf{e_patches}(r).$$

The output matrix **e** of size $3|\mathcal{M}| \times 2$ contains all energy contributions and for any $comp \in \{1, 2\}$

$$\mathbf{e}(n, comp) = \sum_{r=p_{n-1}+1}^{p_n} \mathbf{e_patches}(r) = \mathbf{cs}(p_n) - \mathbf{cs}(p_{n-1}). \quad (24)$$

Note that the vector **e_patches** changes its value inside the loop over components *comp*. Therefore, the whole vector **e** is evaluated at once using the Matlab difference function **diff** with the input vector **indx** of length $3|\mathcal{M}|$, where $\mathbf{indx}(n) = p_n$, $n \in \{1, \dots, d|\mathcal{M}|\}$ with p_n are defined in (14) and additionally (15).

The procedure for the construction of **GG** is listed below:

```

1 function GG = evaluate_GG(patches, v_patches, F)
2 % deformation gradients on patches
3 G = evaluate_F(patches, v_patches);
4
5 % deformation gradient on patches and on 3 components
6 GG = cell(3, 3);
7 GG{1,1} = [G{1,1}; F{1,1}; F{1,1}];
8 GG{1,2} = [G{1,2}; F{1,2}; F{1,2}];

```

```

9  GG{1,3} = [G{1,3}; F{1,3}; F{1,3}];
10 GG{2,1} = [F{2,1}; G{2,1}; F{2,1}];
11 GG{2,2} = [F{2,2}; G{2,2}; F{2,2}];
12 GG{2,3} = [F{2,3}; G{2,3}; F{2,3}];
13 GG{3,1} = [F{3,1}; F{3,1}; G{3,1}];
14 GG{3,2} = [F{3,2}; F{3,2}; G{3,2}];
15 GG{3,3} = [F{3,3}; F{3,3}; G{3,3}];
16 end

```

The cell \mathbf{G} has the same size as \mathbf{F} , but contains the deformation gradient matrices corresponding to the displacements perturbed by ε . The most important feature is using the values of the precomputed input cell \mathbf{F} for the efficient construction of the \mathbf{GG} cell. Note that if the numeric difference step ε is added or subtracted from the first component of displacements, the deformation gradients of the rest two components remains the same and their values are already stored in the \mathbf{F} cell.

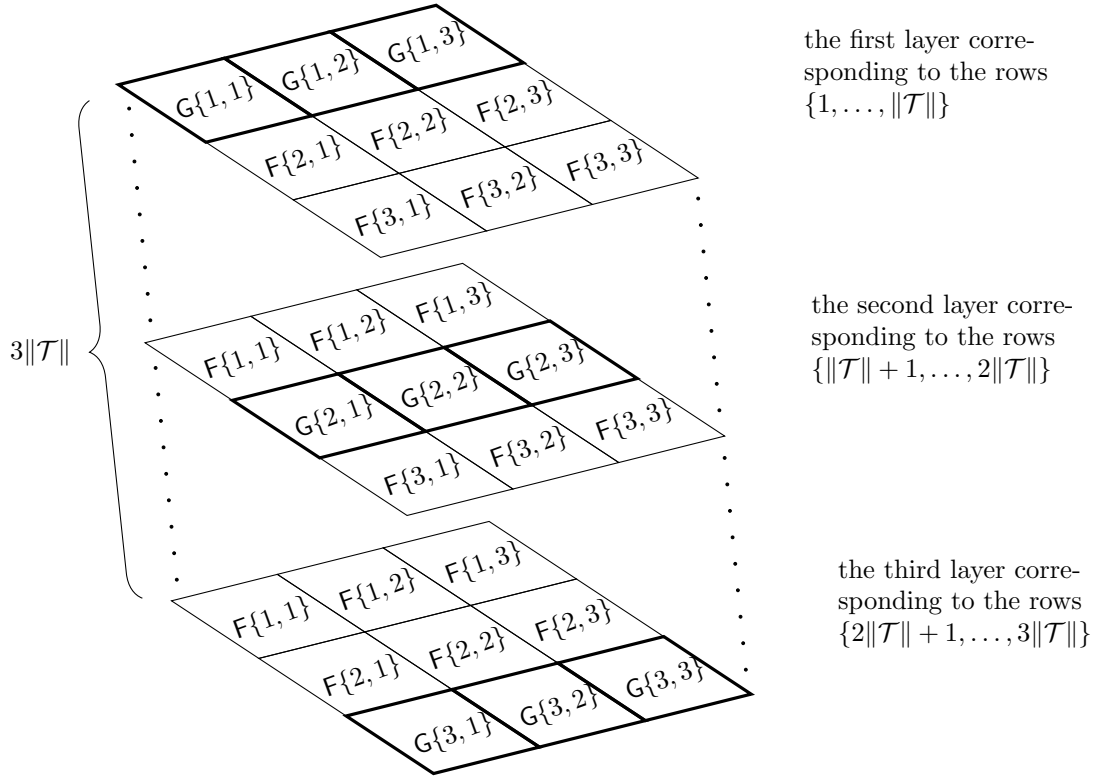


Figure 5: \mathbf{GG} structure of size 3×3 . The three layers are placed vertically.

6.2 Exact approach to evaluate $\nabla J_{grad}(\mathbf{v})$

Evaluation of the exact $\nabla J(\mathbf{v})$ requires explicit deriving of every $\frac{\partial J(\mathbf{v})}{\partial v_n}, n \in \{1, \dots, d|\mathcal{M}|\}$. Gradient of the linear part is trivial and is given by (17). Using (8) one can write

$$\frac{\partial J_{grad}(\mathbf{v})}{\partial v_n} = \sum_{k=1}^{|\mathcal{T}|} |T_k| \frac{\partial}{\partial v_n} W(\mathbf{F}(\mathbf{v})|_{T_k}). \quad (25)$$

Note that the only elements whose energy contributions depend on v_n are those belonging to the i -th patch, where $i = I_{DN}(n)$. Therefore, we can simplify the equation above as

$$\frac{\partial J_{grad}(\mathbf{v})}{\partial v_n} = \sum_{k=1}^{|\mathcal{T}^{(n)}|} |T_k| \frac{\partial}{\partial v_n} W(\mathbf{F}(\mathbf{v})|_{T_k}). \quad (26)$$

By taking (3) and using the chain rule one can write

$$\frac{\partial}{\partial v_n} W(\mathbf{F}(\mathbf{v})) = \sum_{j=1}^d \sum_{m=1}^{dim} \frac{\partial W}{\partial \mathbf{F}_{j,m}}(\mathbf{F}(\mathbf{v})) \frac{\partial \mathbf{F}_{j,m}}{\partial v_n}(\mathbf{v}), \quad (27)$$

where

$$\frac{\partial W(\mathbf{F})}{\partial \mathbf{F}_{j,m}} = C_1 \left(\frac{\partial \mathbf{I}_1(\mathbf{F})}{\partial \mathbf{F}_{j,m}} - \frac{2}{det(\mathbf{F})} \frac{\partial det(\mathbf{F})}{\partial \mathbf{F}_{j,m}} \right) + 2D_1(det(\mathbf{F}) - 1) \frac{\partial det(\mathbf{F})}{\partial \mathbf{F}_{j,m}}. \quad (28)$$

Using the row or column expansion rule for calculating the determinant of a 3×3 matrix, one can express

$$\frac{\partial det(\mathbf{F})}{\partial \mathbf{F}_{j,m}} = (-1)^{j+m} det(\mathbf{F}_{j,m}^{sub}), \quad (29)$$

where $\mathbf{F}_{j,m}^{sub}$ is a 2×2 submatrix of \mathbf{F} given by dropping the j -th row and the m -th column of \mathbf{F} . Furthermore $\frac{\partial \mathbf{I}_1}{\partial \mathbf{F}_{j,m}}$ can be also simplified by

$$\frac{\partial \mathbf{I}_1(\mathbf{F})}{\partial \mathbf{F}_{j,m}} = 2\mathbf{F}_{j,m} \quad (30)$$

From Subsection 6.1 we already know how to assemble $\mathbf{v}|_{T_k}$ and $\mathbf{F}(\mathbf{v})|_{T_k}$. Here, in addition, we need to express $\frac{\partial \mathbf{I}_1(\mathbf{F})}{\partial \mathbf{F}}$, $\frac{\partial det(\mathbf{F})}{\partial \mathbf{F}}$ and $\frac{\partial \mathbf{F}}{\partial v_n}$.

Similarly to the numeric gradient evaluation, the exact gradient evaluation procedure uses the same precomputed structures **v_cell**, **v_elems** and **F_elems**.

```

1 % components of deformation
2 v_cell = createCellFromVector(v, mesh.dim);
3 % components of deformation on elements
4 v_elems = CellAtMatrixOfIndices(v_cell, mesh elems2nodes);
5 % deformation gradients on elements
6 F_elems = evaluate_F(mesh, v_elems);

```

The main procedure for the exact gradient evaluation is provided below:

```

1 % deformations on patches
2 v_patches = CellAtMatrixOfIndices(v_cell, patches elems2nodes);
3 % deformation gradients on patches
4 F_patches = CellAtMatrixOfIndices(F_elems, patches elems);
5
6 % deformation gradients of perturbation
7 GG = evaluate_GG(patches, v_patches, F_patches);
8
9 % densities
10 D_densities_patches = density_D_GradientVector_3D(GG, D_F, params);
11 % energies

```

```

12 D_e_patches = [ patches.volumes; patches.volumes; patches.volumes ]. *
    D_densities_patches;
13 % final energy values on patches
14 csDep = cumsum(D_e_patches);
15 g = zeros(3*numel(nodesMinim),1);
16 g([1:3:end 2:3:end 3:3:end]) = [csDep(indx(1)); diff(csDep(indx))];
17 g = g(dofsMinim_local);

```

Here, **D_densities_patches** is a vector of size $3\|\mathcal{T}\| \times 1$ containing all $\frac{\partial W(\mathbf{F}(\mathbf{v}))}{\partial v_n}$ for every $n \in \{1, \dots, d|\mathcal{M}|\}$ given by (27). Note that the function **density_D.GradientVector_3D** uses the input 3×3 cell structure **D_F_patches**, where $\mathbf{D_F_patches}\{j, m\}(n) = \frac{\partial \mathbf{F}_{j,m}}{\partial v_n}$.

Benchmark 3 *The script `benchmark3.m` evaluates approximation of $\nabla J_{grad}(\mathbf{v})$ on a sequence of uniform mesh refinements defined in Benchmark 2. In order to provide higher accuracy of measure evaluation times, the energies are recomputed 10 times. Table 3 provide evaluation times of gradient approximations both in exact and numerical case.*

mesh level	number of free dofs	evaluation (10x) of exact $\nabla J(\mathbf{v})$: time [s]	evaluation (10x) of num. $\nabla J(\mathbf{v})$: time [s]
1	2133	0.13	0.10
2	11925	0.22	0.31
3	77517	1.73	2.44
4	554013	15.15	20.17
5	4178493	775.91	929.61

Table 3: Benchmark 3 - energy gradient evaluation times in 3D.

7 Application to practical energy minimizations

For a practical energy minimization, the trust-region method [3] available in the MATLAB Optimization Toolbox is utilized. The method also allow to specify a sparsity pattern of the Hessian matrix $\nabla^2 J(v)$ in free degrees of freedom, i.e., only positions (indices) of nonzero entries. The sparsity pattern is directly given by a finite element discretization.

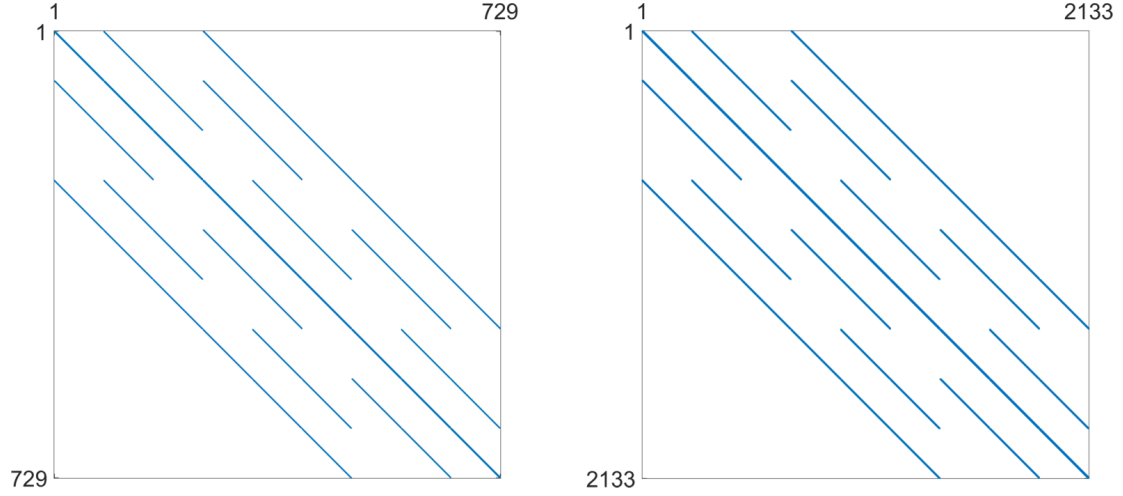


Figure 6: The sparsity pattern of the 3D bar domain based on nodes connectivity (left) and its extension to the vector problem.

Example 2 The sparsity pattern related to the 3D bar domain of Fig. 2 is displayed in Fig. 6 (left). It corresponds to the FEM mesh not taking Dirichlet boundary conditions into account. Therefore it is of size 729×729 . In practical computing, it is first extended from a scalar to vector problem and then restricted to '`mesh.dofsMinim`' indices (right). Since there are 18 Dirichlet nodes fixed in all three directions, the corresponding number of rows and columns of the right hessian sparsity pattern is $(729 - 18) * 3 = 2133$.

7.1 Benchmark 4: time-dependent hyperelasticity in 3D

We consider the elastic bar specified in Benchmark 2 with a time-dependent nonhomogeneous Dirichlet boundary conditions on the right wall. The torsion of the right wall is described by the formula (18) for $x = 0.4$, where the rotation angle is assumed to be a time dependent function $\alpha = \alpha(t) = \alpha_{max}t/T$ for the sequence of integer discrete times $t \in \{1, 2, \dots, T\}$, the final time $T = 24$ and $\alpha_{max} = 8\pi$ being the maximal angle of rotation and ensuring four full rotations of the right Dirichlet wall around the x-axis. Altogether we solve a sequence of T minimization problems (1) with the Neo-Hook energy density (3) and no loading.

The trust-region method also accepts an initial approximation. For the first discrete time we run iterations from the identity $v(x) = x, x \in \Omega$ and for the next discrete time the minimizer of the previous discrete time problem serves as its initial approximation. We output the found energy minimizer for each minimization problem with some minimizers shown in form of deformed meshes in Figure 7. Additionally, we also provide the minimization time, the number of the trust-region iterations and the value of the corresponding minimal energy.

The overall performance is explained in Table 4 for separate computations on level 1, 2 a 3 tetrahedral meshes. We notice that minimizations of finer meshes require only slightly higher number of iterations, which is acceptable. Comparison of energy values $J_{grad}(\mathbf{v})$ indicates convergence of energies of minimizers.

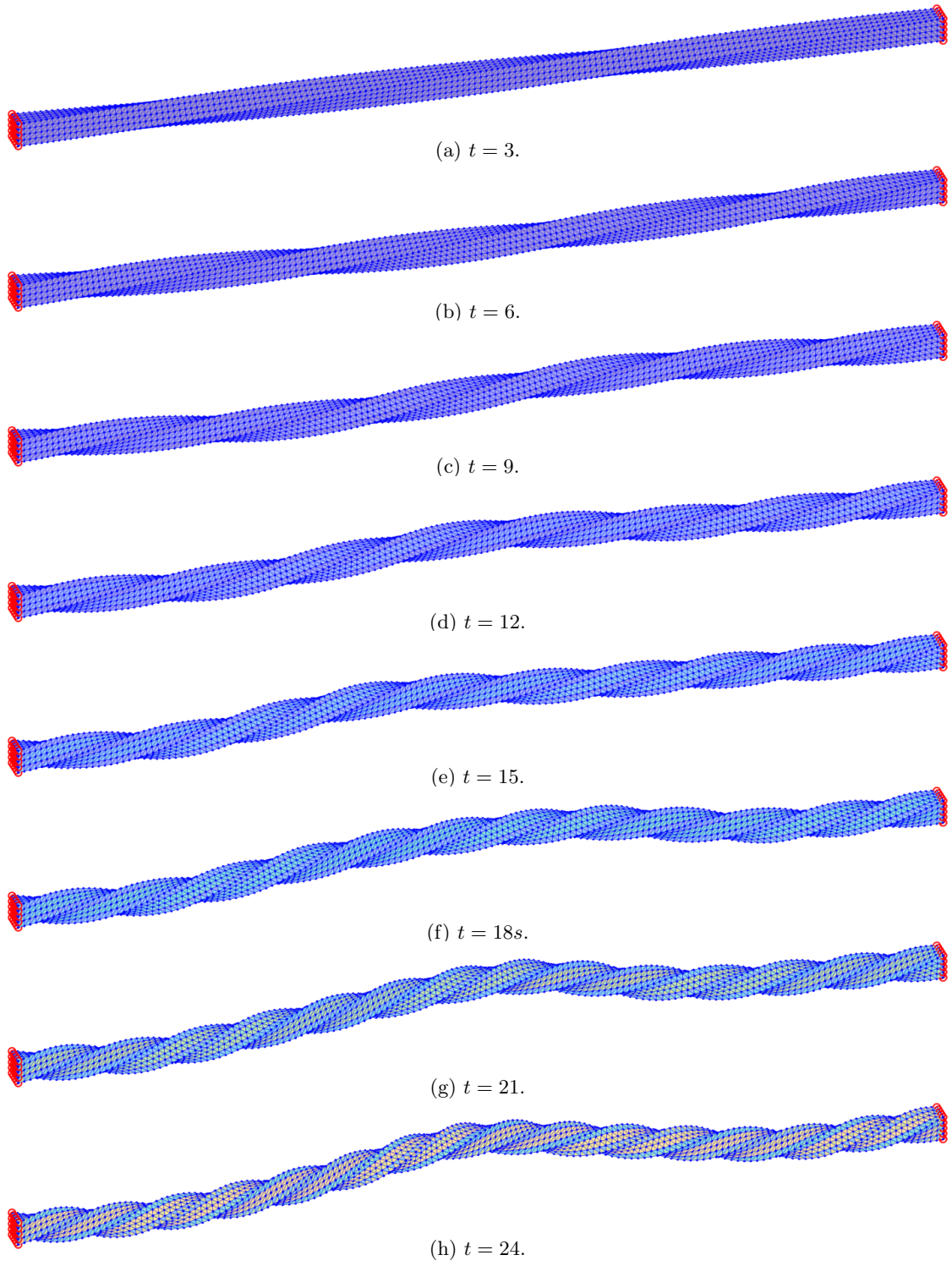


Figure 7: Benchmark 4 - deformation of the tetrahedral mesh subjected to the right time-rotating Dirichlet plane with the underlying Neo-Hookean density.

	level 1, 2133 free dofs			level 2, 11925 free dofs			level 3, 77517 free dofs		
step	time [s]	iters	$J_{grad}(\mathbf{u})$	time [s]	iters	$J_{grad}(\mathbf{u})$	time [s]	iters	$J_{grad}(\mathbf{u})$
t=1	6.54	38	3.46e-01	69.90	50	2.03e-01	1217.20	52	1.63e-01
t=2	7.10	40	1.39e+00	63.47	45	8.11e-01	1316.69	54	6.50e-01
t=3	6.98	40	3.12e+00	67.23	47	1.82e+00	2338.79	93	1.46e+00
t=4	9.65	53	5.54e+00	128.82	80	3.24e+00	1881.69	78	2.60e+00
t=5	8.29	46	8.65e+00	74.59	51	5.07e+00	1504.60	65	4.06e+00
t=6	10.90	60	1.24e+01	119.31	76	7.30e+00	1573.43	68	5.85e+00
t=7	8.92	49	1.69e+01	117.09	76	9.93e+00	1553.47	68	7.97e+00
t=8	12.04	64	2.21e+01	113.91	75	1.30e+01	1370.54	61	1.04e+01
t=9	11.09	60	2.79e+01	129.04	85	1.64e+01	1628.20	73	1.32e+01
t=10	13.72	74	3.44e+01	151.79	100	2.03e+01	1437.58	68	1.63e+01
t=11	11.85	64	4.16e+01	140.85	93	2.45e+01	1293.81	58	1.97e+01
t=12	19.54	104	4.96e+01	101.00	68	2.92e+01	1458.76	65	2.34e+01
t=13	13.00	70	5.81e+01	116.78	78	3.42e+01	1536.07	69	2.75e+01
t=14	10.31	55	6.74e+01	81.73	55	3.97e+01	1343.79	61	3.19e+01
t=15	15.06	81	7.74e+01	127.74	87	4.56e+01	1276.29	58	3.66e+01
t=16	16.40	89	8.80e+01	155.09	106	5.18e+01	1495.50	68	4.17e+01
t=17	30.81	167	9.93e+01	183.67	125	5.85e+01	1477.35	68	4.71e+01
t=18	17.90	97	1.11e+02	110.20	75	6.55e+01	1654.44	76	5.28e+01
t=19	20.98	114	1.24e+02	87.38	59	7.30e+01	1363.82	62	5.88e+01
t=20	18.88	102	1.37e+02	96.01	65	8.09e+01	1733.22	83	6.52e+01
t=21	15.13	82	1.51e+02	75.25	51	8.92e+01	6389.93	290	7.18e+01
t=22	16.48	89	1.66e+02	100.68	69	9.78e+01	1892.99	82	7.88e+01
t=23	10.50	57	1.82e+02	100.51	69	1.07e+02	2040.18	89	8.61e+01
t=24	16.79	91	1.98e+02	91.50	63	1.16e+02	2983.90	131	9.37e+01

Table 4: Benchmark 4 - performance of hyperelasticity minimizations in 3D.

7.2 Benchmarks 5 and 6: hyperelasticity and p-Laplacian in 2D

Although our exposition is mainly focused on implementation details in 3D, a reduction to 2D ($dim = 2$) is straightforward.

As the first example we consider a square domain with lengths $lx = ly = 2$ perforated by a hole with radius $r = 1/3$ (Fig. 8 left) and whose center is located at the center of the square, subjected to the zero Dirichlet condition on the bottom and left edges, a constant loading $\mathbf{f}(\mathbf{x}) = (-4 \cdot 10^7, -4 \cdot 10^7)$ and the elastic parameters specified in Benchmark 2. The resulting deformation and the deformation gradient densities are depicted in Fig. 8 (right).

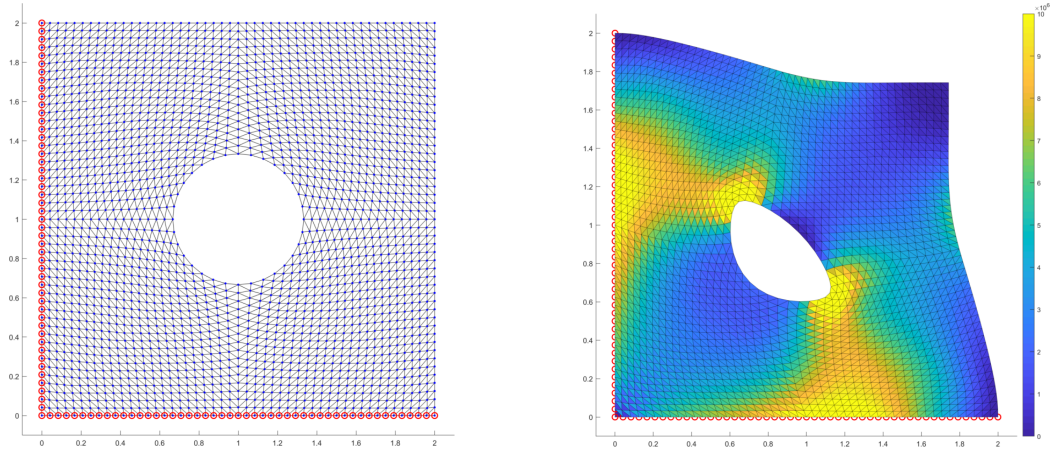


Figure 8: Benchmark 5 - a triangulation of the square domain perforated by a hole (left) and its deformation with the underlying Neo-Hookean density (right).

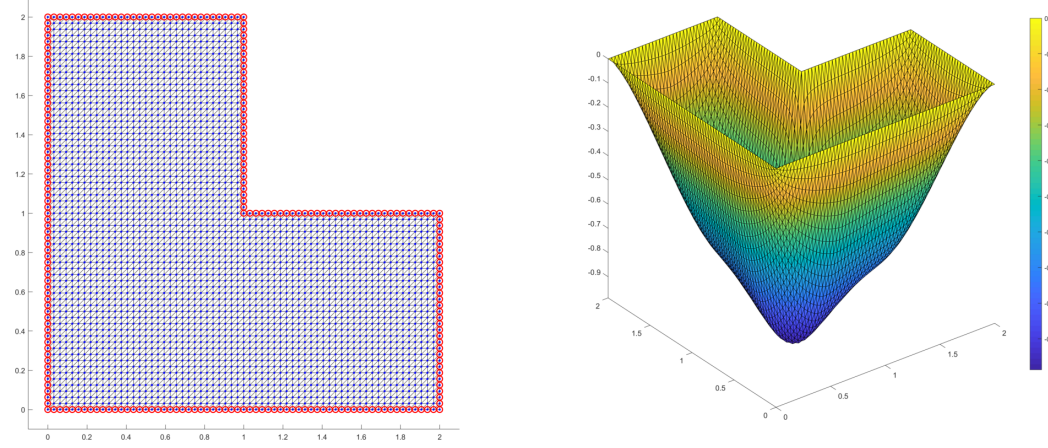


Figure 9: Benchmark 6 - a triangulation of the L-shape domain (left) and the solution p-Laplacian for the power $p = 3$ and a constant loading $f(\mathbf{x}) = -10$ (right).

As the second example we provide performance details minimization of the p-Laplacian energy functional (4) over the L-shape domain (Fig. 9 left). The constant loading $f = -10$ is assumed together with zero Dirichlet boundary conditions on the domain boundary. The solution is displayed in Fig. 9 (right). Table 6 depicts performance of all options for the power $p = 3$. The results confirm faster evaluation times then in our former contribution [11]. This is mainly due to improved vectorization concepts here, due to the faster CPU and finally due to update of the trust-region in-built implementation in the latest version of Matlab.

7.3 Final implementation remarks

Assembly times in all benchmarks were obtained on a MacBook Air (M1 processor, 2020) with 16 GB memory. Our MATLAB implementation is available at

<https://www.mathworks.com/matlabcentral/fileexchange/97889>

level	free dofs	exact gradient			numerical gradient		
		time [s]	iters	$J(\mathbf{u})$	time [s]	iters	$J(\mathbf{u})$
1	278	0.06	6	27.8870	0.08	6	27.8870
2	1102	0.15	6	27.6292	0.20	6	27.6292
3	4382	0.57	6	27.5563	0.69	6	27.5563
4	17470	3.26	8	27.5362	3.72	8	27.5362
5	69758	51.79	36	27.5178	62.55	40	27.5178

Table 5: Benchmark 5 - performance of hyperelasticity minimizations in 2D.

level	free dofs	exact gradient			numerical gradient		
		time [s]	iters	$J(\mathbf{u})$	time [s]	iters	$J(\mathbf{u})$
1	33	0.02	10	-7.5353	0.03	10	-7.5353
2	161	0.06	13	-7.9729	0.10	12	-7.9729
3	705	0.12	13	-8.1039	0.21	12	-8.1039
4	2945	0.34	13	-8.1445	0.50	11	-8.1445
5	12033	1.36	13	-8.1578	2.10	12	-8.1578
6	48641	6.95	14	-8.1625	12.56	17	-8.1625
7	195585	52.75	15	-8.1642	78.56	19	-8.1642
8	784385	645.22	24	-8.1649	754.91	24	-8.1649

Table 6: Benchmark 6 - performance of p-Laplacian minimizations for $p = 3$ in 2D.

for download and testing. It is based on own codes [2, 5, 13] used primarily for assemblies of finite element matrices. It also uses the function **mc colon** from the reservoir simulator [9]. The names of mesh attributes were initially motivated by codes of [1] and further modified. The code is designed in a modular way that different scalar and vector problems involving the first gradient energy terms can be easily added.

Acknowledgement

A. Moskovka was supported by the Strategy 21 of the CAS, program 23: City as a Laboratory of Change Historical Heritage and Place for Safe and Quality Life and by the R&D project 8J21AT001 Model Reduction and Optimal Control in Thermomechanics. J. Valdman announces the suport of the Czech Science Foundation (GACR) through the grant GF19-29646L Large Strain Challenges in Materials Science.

References

- [1] J. Albery, C. Carstensen, S. Funken: *Remarks around 50 lines of Matlab: short finite element implementation*, Numerical Algorithms 20, 1999, 117-137.
- [2] I. Anjam, J. Valdman: *Fast MATLAB assembly of FEM matrices in 2D and 3D: edge elements*, Applied Mathematics and Computation, 2015, 267, 252–263.
- [3] A.R. Conn, N.I.M. Gould, P.L. Toint: *Trust-Region Methods*. SIAM, Philadelphia, 2000.
- [4] P.G. Ciarlet: *The Finite Element Method for Elliptic Problems*, SIAM, Philadelphia, 2002.
- [5] M. Čermák, S. Sysala, J. Valdman: *Efficient and flexible MATLAB implementation of 2D and 3D elastoplastic problems*, Applied Mathematics and Computation, 2019, 355, 595-614.

- [6] P. Drábek, J. Milota: *Methods of Nonlinear Analysis: Applications to Differential Equations* (second edition), Birkhauser, 2013.
- [7] J. Koko: *Fast MATLAB assembly of FEM matrices in 2D and 3D using cell-array approach*, International Journal of Modeling, Simulation, and Scientific Computing Vol. 7, No. 3 (2016).
- [8] M. Kružík, T. Roubíček: *Mathematical Methods in Continuum Mechanics of Solids*, Springer, 2019.
- [9] K. A. Lie: *An introduction to reservoir simulation using MATLAB: User guide for the Matlab Reservoir Simulation Toolbox (MRST)*, Technical report, SINTEF ICT, December 2016. (<http://www.sintef.no/projectweb/mrst/>).
- [10] J. E. Marsden, T. J.R. Hughes: *Mathematical foundations of elasticity*, Dover Publications, 1994.
- [11] C. Matonoha, A. Moskovka, J. Valdman: *Minimization of p -Laplacian via the Finite Element Method in MATLAB*, arXiv:2103.02125v2.
- [12] MATLAB documentation to Minimization with Gradient and Hessian Sparsity Pattern, <https://www.mathworks.com/help/optim/ug/minimization-with-gradient-and-hessian-sparsity-pattern.html> .
- [13] T. Rahman, J. Valdman: *Fast MATLAB assembly of FEM matrices in 2D and 3D: nodal elements*, Applied Mathematics and Computation, 2013, 219, 7151-7158.
- [14] H. P. Langtangen: *Basic finite element methods*, 12.12.2012.
- [15] T. Weinberg, B. Sousedík: *Fast implementation of mixed RT0 finite elements in MATLAB*, SIAM Undergraduate Research Online, Volume 12, 2018.